

7 Tesla quantitative hip MRI: T1, T2 and T2* mapping of hip cartilage in healthy volunteers

Andrea Lazik¹ · Jens M. Theysohn¹ · Christina Geis¹ · Sören Johst² · Mark E. Ladd^{1,2,3} · Harald H. Quick^{2,4} · Oliver Kraff²

Received: 1 April 2015 / Revised: 28 July 2015 / Accepted: 3 August 2015 / Published online: 28 August 2015
© European Society of Radiology 2015

Abstract

Objectives To evaluate the technical feasibility and applicability of quantitative MR techniques (delayed gadolinium-enhanced MRI of cartilage (dGEMRIC), T2 mapping, T2* mapping) at 7 T MRI for assessing hip cartilage.

Methods Hips of 11 healthy volunteers were examined at 7 T MRI with an 8-channel radiofrequency transmit/receive body coil using multi-echo sequences for T2 and T2* mapping and a dual flip angle gradient-echo sequence before (T1₀) and after intravenous contrast agent administration (T1_{Gd}; 0.2 mmol/kg Gd-DTPA²⁻ followed by 0.5 h of walking and 0.5 h of rest) for dGEMRIC. Relaxation times of cartilage were measured manually in 10 regions of interest. Pearson's correlations between R1_{delta}=1/T1_{Gd}-1/T1₀ and T1_{Gd} and between T2 and T2* were calculated. Image quality and the delineation of acetabular and femoral cartilage in the relaxation time maps were evaluated using discrete rating scales.

Results High correlations were found between R1_{delta} and T1_{Gd} and between T2 and T2* relaxation times (all $p < 0.01$). All techniques delivered diagnostic image quality, with best

delineation of femoral and acetabular cartilage in the T2* maps (mean 3.2 out of a maximum of 4 points).

Conclusions T1, T2 and T2* mapping of hip cartilage with diagnostic image quality is feasible at 7 T. To perform dGEMRIC at 7 T, pre-contrast T1 mapping can be omitted.

Key Points

- dGEMRIC of hip cartilage with diagnostic image quality is feasible at 7 T.
- To perform dGEMRIC at 7 T, pre-contrast T1 mapping can be omitted.
- T2(*) mapping of hip cartilage with diagnostic image quality is feasible at 7 T.
- T2 and T2* relaxation times of cartilage were highly correlated at 7 T.
- Best delineation of femoral and acetabular cartilage was found in T2* maps.

Keywords Ultra-high-field MRI · Hip cartilage · dGEMRIC · T2 mapping · T2* mapping

Abbreviations

BMI	body mass index
dGEMRIC	delayed gadolinium-enhanced MRI of cartilage
DREAM	dual refocusing echo acquisition mode
FOV	field of view
FLASH	fast low angle shot
MRI	magnetic resonance imaging
RF	radiofrequency
ROI	region of interest
SAR	specific absorption rate
SD	standard deviation
SNR	signal-to-noise ratio
T	Tesla
TI	inversion time

✉ Andrea Lazik
andrea.lazik@uk-essen.de

¹ Department of Diagnostic and Interventional Radiology and Neuroradiology, University Hospital Essen, Hufelandstr. 55, 45147 Essen, Germany

² Erwin L. Hahn Institute for Magnetic Resonance Imaging, University of Duisburg-Essen, Essen, Germany

³ Medical Physics in Radiology, German Cancer Research Center (DKFZ), Heidelberg, Germany

⁴ High Field and Hybrid MR Imaging, University Hospital Essen, Essen, Germany

TE	echo time
TR	repetition time
UHF	ultra-high field

Introduction

Magnetic resonance imaging (MRI) plays an important role in the non-invasive staging of osteoarthritis, as well as in the diagnosis of focal cartilage lesions [1] and their postoperative follow-up [2]. Traditional anatomical imaging techniques can provide information about cartilage morphology, whereas quantitative imaging methods are able to show subtle changes in cartilage composition even before structural changes appear. Among them, T2 and T2* mapping techniques provide information about the collagen structure [3], whereas delayed gadolinium-enhanced MRI of cartilage (dGEMRIC), a T1 mapping technique after intravenous application of negatively charged contrast agent, provides information about the glycosaminoglycan content in cartilage [4, 5]. The use of quantitative imaging methods has emerged during recent years, especially against the background of increasingly utilized hip-preserving, regenerative therapies [6].

Especially in the hip, high spatial resolution is needed for adequate quantitative as well as qualitative cartilage imaging, mainly as a result of the thinner cartilage layer and the spherical shape of the joint compared to the knee [7]. MRI at 7 Tesla (T), with its inherently higher signal-to-noise ratio (SNR) compared to clinical field strengths of 1.5 T or 3 T, allows to invest SNR in increased spatial resolution and is thus expected to improve diagnostic accuracy in such demanding applications [8]. However, imaging at ultra-high-field strengths (UHF, ≥ 7 T) remains challenging. These challenges include increased power deposition in the examined tissue, characterized by the specific absorption rate (SAR) [9] on the one hand, and limited available radiofrequency (RF) peak power and hence decreased penetration depth on the other hand. Another factor complicating imaging at UHF is B_1 field heterogeneity, resulting in the need for dedicated RF shims to achieve homogenous excitation in the region of interest [10, 11]. These RF issues are emphasized when imaging larger fields of view (FOV) or deep anatomical regions like the hip. Furthermore, just recently a limited number of commercially available surface coils for imaging the body at 7 T have become available, mostly prototype RF coils distributed through spinoff companies from other 7 T sites, resulting in the need to develop those individually [12].

Despite these challenges, imaging the hip joint at 7 T MRI has been successfully shown by Ellermann et al. [13]. Furthermore, Chang et al. [14] and Theysohn et al. [15, 16] established high-resolution anatomical MR sequences at 7 T with a focus on qualitative cartilage depiction. However, quantitative MR techniques at 7 T, as applied for analysing knee cartilage by several authors [17–20], have, to our knowledge, not yet been applied in the hip.

Therefore, the aim of this study was to evaluate the technical feasibility and the applicability of quantitative MR techniques at 7 T MRI for imaging hip cartilage.

Materials and methods

Study population

Approval from the local institutional ethics committee was gained prior to the study. Exclusion criteria were collected anamnestically and defined as current or previous hip pain, previous hip surgeries, risk of having renal insufficiency (assessed anamnestically, including any history of renal disease (i.e. dialysis, transplantation, single kidney, kidney surgery or cancer), diabetes and hypertension), implants incompatible with 7 T MRI as well as claustrophobia. After signing informed consent, unilateral hip-joint imaging was performed on 11 healthy volunteers (5 female, 6 male; 21–46 years, mean 27.0, SD 7.3; body mass index (BMI) 18.7–26.6 kg/m², mean 22.5, SD 3.1) and, exemplarily, in one patient 10 months after acetabular cartilage transplantation. Two further volunteers were excluded because of claustrophobia.

MR system and RF transmitter adjustments

All MR imaging was performed on a 7 T research whole-body MR system (Magnetom 7 T, Siemens Healthcare GmbH, Germany) using an in-house-developed 8-channel RF transmit/receive body coil consisting of two arrays with four elements each placed ventrally and dorsally on the pelvis.

For B_1 homogenization, the second-order circularly polarized (CP2+) transmit mode utilizing phase increments of 90° between the eight transmit channels was used as a fixed RF shim setting for all subjects. This RF mode had previously proved superior to individual RF shimming in hip imaging at 7 T in terms of workflow and maximum allowed input power in compliance with safety guidelines [15]. A 3D fast low angle shot (FLASH) sequence was used to verify the successful shift of signal dropouts medially away from the hip joint prior to the study protocol. Additionally, maps of the flip angle distribution were obtained by fast B_1^+ mapping using dual refocusing echo acquisition mode (DREAM) [21]. Parameters of the DREAM sequence were FOV 160 × 160 mm², matrix 64 × 64, slice thickness 5 mm, TR 6.3 ms, TE 1.98/3.95 ms, preparation flip angle 60° and acquisition time 7.5 s. This technique had performed superior to other established B_1^+ mapping techniques in a previous study [22]. As quantitative imaging is prone to flip angle variations [23, 24], the flip angle maps were used to perform adjustments of the RF transmit power. Transmit voltages were calculated to achieve the desired mean flip angle in the joint and were subsequently applied for the quantitative imaging sequences.

T1 mapping

A 3D spoiled fast gradient-echo (3D FLASH) sequence (TR 15 ms, TE 2.73 ms) with two different excitation flip angles of 3° and 18° was used to assess the T1 relaxation times $T1_0$ [25, 26]. Images were acquired in a sagittal view with a FOV of $160 \times 160 \text{ mm}^2$, a matrix of 448×448 and a slice thickness of 2 mm. Further parameters are shown in Table 1.

T1 was extracted from a linear fit $T1 = -TR/m$, where m is the slope between two measurement points obtained by arranging $S(\alpha)/\sin(\alpha)$ versus $S(\alpha)/\tan(\alpha)$, with $S(\alpha)$ being the FLASH signal intensity of the data set obtained with the applied flip angle α . This post-processing was done using vendor-provided software (Syngo MapIt, Siemens AG, Healthcare Sector, Germany), resulting in a colour-coded map of T1 relaxation times.

T1 mapping was repeated with the same technique after contrast agent administration ($T1_{Gd}$) as part of a dGEMRIC protocol [5]: after leaving the MR system, volunteers received $Gd-DTPA^{2-}$ (Magnevist, Bayer Healthcare, Leverkusen, Germany) intravenously with a concentration of 0.2 mmol/kg body weight and were asked to perform 0.5 h of walking and 0.5 h of rest. Subsequently, the volunteers were repositioned in the MR system to acquire contrast-enhanced T1 mapping measurements 71–97 min (mean 81 min, SD 6.5) after contrast agent administration.

In five subjects (three before and two after contrast agent administration), T1 relaxation times were additionally assessed via an inversion recovery sequence (TR 6000 ms, TE 6.1 ms) with six TI times (200, 500, 600, 800, 1000, 1200 ms) applied in a single central slice of the hip joint in

sagittal view (FOV $160 \times 160 \text{ mm}^2$, matrix 192×154 , slice thickness 5 mm). T1 was calculated as $T1_{\text{calc}} = TI_{\text{zero}} / \ln 2$, with TI_{zero} being the inversion time with the lowest signal intensity in cartilage.

T2 and T2* mapping

Subsequent to the unenhanced T1 measurements, multi-contrast spin-echo and gradient-echo sequences with five echoes each were applied for T2 and T2* mapping in sagittal view (FOV $160 \times 160 \text{ mm}^2$, matrix 320×320 , slice thickness 2.5 mm). Echo times used were 10.1, 20.2, 30.3, 40.4 and 50.5 ms for T2 mapping (TR 1500 ms) and 3.06, 8.0, 12.94, 17.88 and 22.82 ms for T2* mapping (TR 130 ms). Further sequence parameters are given in Table 1. As volunteers rested for at least 0.5 h prior to the measurement of T2 and T2* relaxation times, influences of joint loading were minimized. Colour-coded maps were calculated manually (Syngo MapIt, Siemens Healthcare GmbH, Germany) after reviewing the consistency of signal decrease with TE using Syngo MeanCurve (Siemens Healthcare GmbH, Germany). In case of an inconsistent signal decrease, images from the first echo were not considered for calculating the map.

MRI evaluation

A qualitative analysis, which was performed in consensus by two radiologists, focused on the delineation of acetabular and femoral cartilage (four-point scale: 1=not delineable, 2=partly delineable, 3=largely delineable, 4=fully delineable) in the calculated relaxation time maps of the volunteers. A mean score of more than 2.5 points was considered suitable for diagnostic imaging. Additionally, the source images were evaluated regarding the homogeneity of the signal in the hip-joint region (three-point scale: 1=severe heterogeneities, 2=moderate heterogeneities, 3=no heterogeneities) and regarding artefacts affecting image quality (three-point-scale: 1=severe artefacts, 2=moderate artefacts, 3=no artefacts).

T1, T2 and T2* relaxation times were measured by manually drawing regions of interest (ROIs) in five defined regions in both acetabular and femoral cartilage of the volunteers: three ROIs were placed centrally as well as ventrally and dorsally in a sagittal slice showing the central region of the femoral head. Two additional central ROIs were placed 5–10 mm laterally and medially from this slice (Fig. 1). The ROIs covered the whole cartilage thickness in each region.

For test reproducibility, the central acetabular ROI in the central slice was drawn again at least 6 weeks later by the same radiologist as well as by a second reader. Both had knowledge of the previously analysed slice position, but were not aware of either the exact position or the shape of the ROI.

Table 1 Sequence parameters

	T1 mapping	T2 mapping	T2* mapping
Sequence type	Gradient echo	Spin echo	Gradient echo
TR (ms)	15.0	1500	130
TE (ms)	2.73	10.1–50.5	3.06–22.82
FOV (mm)	160	160	160
In-plane resolution (mm^2)	0.4×0.4	0.5×0.5	0.5×0.5
Slice thickness (mm)	2	2.5	2.5
Slice resolution (%)	77	100	100
Number of slices	40	5	5
Phase encoding direction	AP	AP	AP
Bandwidth (Hz/pixel)	280	401	500
PAT	2 (GRAPPA)	2 (GRAPPA)	None
Averages	1	1	2
Acquisition time (min)	5:13	4:53	2:06

All sequences were applied in sagittal orientation

TR repetition time, TE echo time, FOV field of view, PAT parallel acquisition technique, GRAPPA generalized autocalibration with partially parallel acquisition

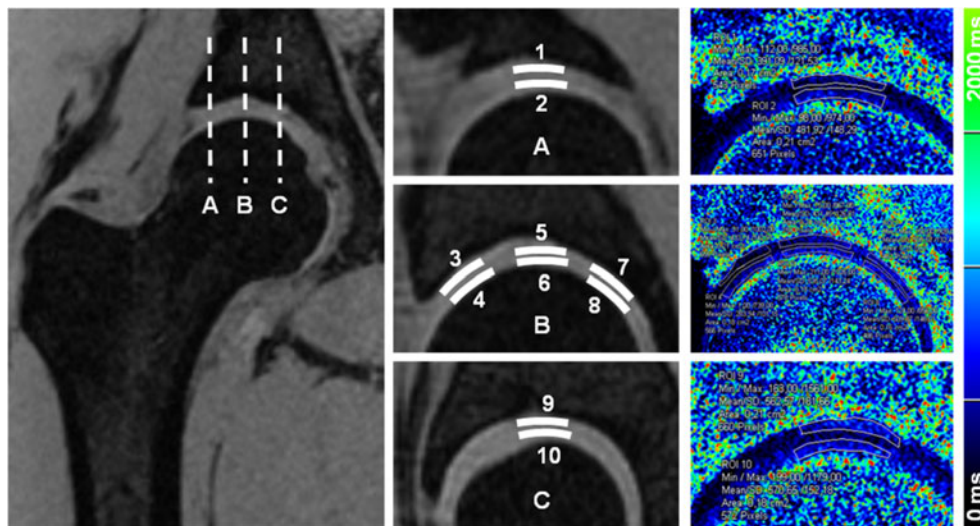


Fig. 1 *Left and middle column* Overview of the cartilage regions of interest (ROI) (white bars) used for measuring the relaxation times, displayed in a fat suppressed T1w VIBE sequence acquired at 3 T. In the central sagittal slice (B), three ROIs were placed (centrally, ventrally, dorsally), each in the acetabular and femoral cartilage. In a slice 5–10 mm medial (A) and lateral (C) of the central slice, a ROI was placed centrally both in the acetabular and femoral cartilage. For further evaluations, the

analysed cartilage regions were numbered as shown in A, B and C (1 acetabulum lateral slice, 2 femur lateral slice, 3 acetabulum central slice ventral, 4 femur central slice ventral, 5 acetabulum central slice central, 6 femur central slice central, 7 acetabulum central slice dorsal, 8 femur central slice dorsal, 9 acetabulum medial slice, 10 femur medial slice). *Right column* Example of actual ROI measurements in a contrast-enhanced T1 map of one volunteer

Statistical analysis

Mean values with standard deviations (SD) were calculated for all parameters. Statistical analysis was performed using SPSS Statistics 19 (IBM, USA). A *p* value smaller than 0.05 was considered to be statistically significant. The contrast agent concentration was considered proportional to $[R1_{\text{delta}} = 1/T1_{\text{Gd}} - 1/T1_0]$ and compared to $T1_{\text{Gd}}$ using Pearson's correlation. The T1 relaxation times gained via the inversion recovery sequence were compared to those gained via the dual-flip-angle technique using a paired *t* test. Correlations between the T2 and T2* relaxation times were assessed by Pearson's correlation. Analysis of variance (ANOVA) for repeated measurements was used to calculate significant differences of T1, T2 and T2* relaxation times between the anatomical regions. In the case of significant differences between groups, a post hoc analysis with Bonferroni correction ($n=10$) was performed. Differences between the methods regarding qualitative ratings were calculated using a Wilcoxon sign rank test. Mean bias with 95 % confidence interval (CI) as well as coefficient of variation (CV) was used to assess intra- and inter-reader reproducibility of the measured relaxation times.

Results

T1 mapping

Delineation of femoral and acetabular cartilage was poor in the unenhanced relaxation time maps, but clearly improved

after contrast agent administration to a diagnostically applicable level ($T1_0$: 1–3 points, mean 1.7, SD 0.6; $T1_{\text{Gd}}$: 2–4 points, mean 2.9, SD 0.8; $p=0.10$).

Qualitatively, the signal was fully homogenous at both flip angles of the 3D FLASH sequence, both before and after contrast agent administration (consistently 3 points in every volunteer before and after contrast agent administration, $p=1.0$, Fig. 2a–d). No artefacts were recognized in any of the scans prior to contrast agent administration (mean 3.0 ± 0.0 points). A moderate artefact (2 points) was recognized in only one examination after contrast agent administration owing to the parallel imaging technique applied (Fig. 2i) [27]. The other images of the remaining 10 volunteers received 3 points consistently (mean 2.9 ± 0.3 points). A significant difference between unenhanced and contrast-enhanced images was not observed ($p=0.317$).

Mean size of the evaluated ROIs was 425 pixels. The thickness of the ROIs ranged from 0.10 cm (femur central slice central) to 0.18 cm (acetabulum central slice ventral) corresponding to a mean thickness of 3.2 pixels. Mean values of $T1_0$ were 1508 ± 647 ms (range 346–2780 ms) for acetabular and 1499 ± 633 ms (range 422–2794 ms) for femoral cartilage. Mean values of $T1_{\text{Gd}}$ were 911 ± 449 ms (range 191–2070 ms) for acetabular and 950 ± 455 ms (range 245–1987 ms) for femoral cartilage. There was a high correlation between $R1_{\text{delta}}$ and $T1_{\text{Gd}}$ for both regions ($p < 0.001$, Fig. 3a). The distribution of $T1_0$ and $T1_{\text{Gd}}$ was slightly inhomogeneous over the various cartilage regions evaluated without significant differences or any specific pattern recognized (Fig. 4a).

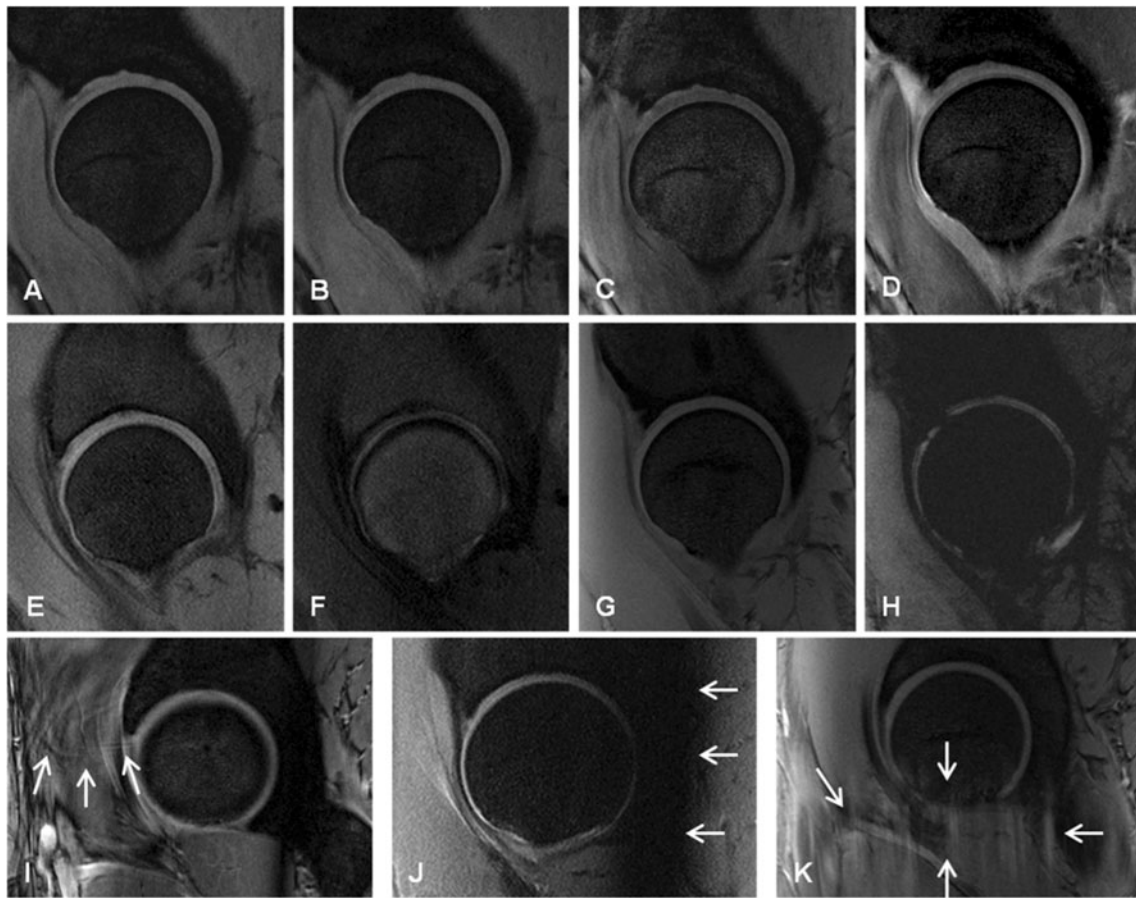


Fig. 2 **a–d** Source images of T1 mapping with flip angles of 3° (**a, c**) and 18° (**b, d**) before (**a, b**) and after (**c, d**) contrast agent administration with best rated image quality regarding signal homogeneity and artefacts (3 points). **e–h** First and last echoes of the T2 mapping sequence (**e** TE=10.1 ms; **f** TE=50.5 ms; TR=1500 ms) in one volunteer and of the T2* mapping sequence (**g** TE=3.06 ms; **h** TE=22.08 ms; TR=130 ms) in another volunteer with best rated image quality regarding signal homogeneity and artefacts (3 points). The signal void in **h**, seen in the

anterosuperior portion of the hip joint, reflects a region of shorter T2* relaxation times compared to adjacent tissue, and was not assessed as artefact. **i–k** Examples of worst rated image quality in source images of **i** T1 mapping (FA 18°): 2 points due to PAT artefact (*arrows*); **j** T2 mapping (TE=20.2 ms): 1 point due to signal heterogeneities affecting the dorsal part of the hip joint region (*arrows*); and **k** T2* mapping (TE=3.06 ms): 2 points due to pulsation artefacts (*arrows*)

Both intra- and inter-reader reliability were excellent (intra-reader reliability: mean bias 53.5 ms (95 % CI –1.2 to 108.3 ms), CV 6.5 %; inter-reader reliability: mean bias 86.2 ms (95 % CI 8.1–163.3 ms), CV 10.4 %).

T1 relaxation times estimated by the use of the inversion recovery sequence were highly comparable to the ones achieved via the fast dual-flip-angle technique: mean values showed high correlation ($p=0.002$) and did not differ significantly ($p=0.86$) (Table 2).

T2 and T2* mapping

Delineation of femoral and acetabular cartilage was clearly diagnostic for both techniques, but slightly better in T2* compared to T2 without statistical significance (T2*: 3–4 points, mean 3.2, SD 0.4; T2: 1–4 points, mean 3.0, SD 1.0; $p=0.763$).

Also, signal homogeneity was better in T2* compared to T2. In T2, severe signal heterogeneities were recognized in two volunteers, masking the dorsal part of the hip joint (Fig. 2j). However, the ventral and central parts of the joint were free of signal heterogeneities in those volunteers. Overall, the score for signal heterogeneities in T2 was 2.5 ± 0.8 points. In T2*, only moderate signal heterogeneities were recognized in two volunteers, resulting in an improved overall score (mean 2.8 ± 0.4 points, Fig. 2e–h). Heterogeneities in T2* were localized to the dorsal part of the sagittal images, hardly affecting the hip-joint region. The difference in signal heterogeneities was statistically significant ($p=0.046$).

No severe artefacts were noticed either in T2 or in T2*, resulting in excellent overall scores (T2: mean 2.8 ± 0.4 points; T2*: mean 2.9 ± 0.3 points, $p=0.317$). Moderate artefacts due to pulsations of the inguinal vessels were noticed in two volunteers in T2 and in only one volunteer in T2* (Fig. 2k).

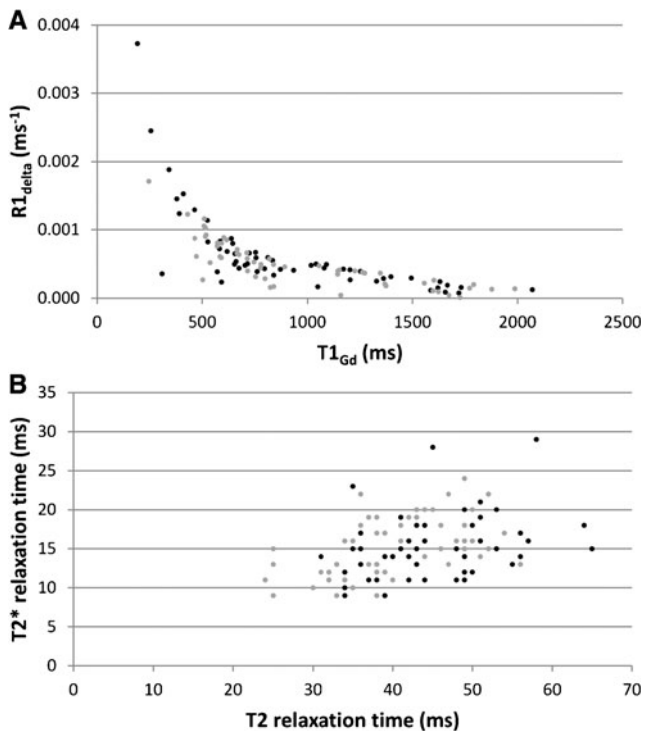


Fig. 3 **a** Correlation of $R1_{\text{delta}}$ and $T1_{\text{Gd}}$ for acetabular (black, $p=10^{-5}$) and femoral (grey, $p=5 \times 10^{-12}$) cartilage. Overall $p=10^{-12}$. **b** Correlation of T2 and $T2^*$ relaxation times for acetabular (black, $p=0.0002$) and femoral (grey, $p=0.009$) cartilage. Overall $p=2 \times 10^{-5}$

Mean size of the evaluated ROIs was 217 pixels both in T2 and $T2^*$. The thickness of the ROIs placed in the T2 maps ranged from 0.11 cm (femur central slice central) to 0.21 cm (acetabulum central slice ventral) corresponding to a mean thickness of 2.9 pixels. The thickness of the ROIs placed in the $T2^*$ maps ranged from 0.08 cm (femur central slice dorsal) to 0.20 cm (acetabulum central slice ventral) corresponding to a mean thickness of 2.6 pixels. T2 relaxation times were 44.5 ± 8.2 ms (range 31–65 ms) for acetabular and 40.7 ± 7.9 ms (range 24–56 ms) for femoral cartilage. $T2^*$ relaxation times were 15.2 ± 4.1 ms (range 9–29 ms) for acetabular and 15.3 ± 3.8 ms (range 9–24 ms) for femoral cartilage. There was high correlation between T2 and $T2^*$ relaxation times (acetabular: $p=0.009$, femoral: $p=0.0002$, Fig. 3b). The distribution of T2 and $T2^*$ relaxation times was slightly inhomogeneous over the different evaluated cartilage regions (Fig. 4b) with significant differences between the regions both for T2 and $T2^*$ (ANOVA: both $p < 0.001$). Post hoc analysis revealed significant differences being between the regions 2/5 ($p=0.013$), 2/7 ($p=0.004$), 2/8 ($p=0.032$), 3/7 ($p=0.016$), 6/7 ($p=0.031$) and 7/9 ($p=0.001$) for T2 and between the regions 1/8 ($p=0.012$), 2/4 ($p=0.027$), 2/7 ($p=0.007$), 2/8 ($p < 0.001$), 2/10 ($p=0.017$) and 6/8 ($p=0.04$) for $T2^*$.

Both intra- and inter-reader reliability were excellent for T2 (intra-reader reliability: mean bias -0.6 ms (95 % CI -3.2 to 2.0 ms), CV 7 %; inter-reader reliability: mean bias 0.2 ms (95 % CI -2.3 to 2.7 ms), CV 8.5 %) and also for $T2^*$ (intra-

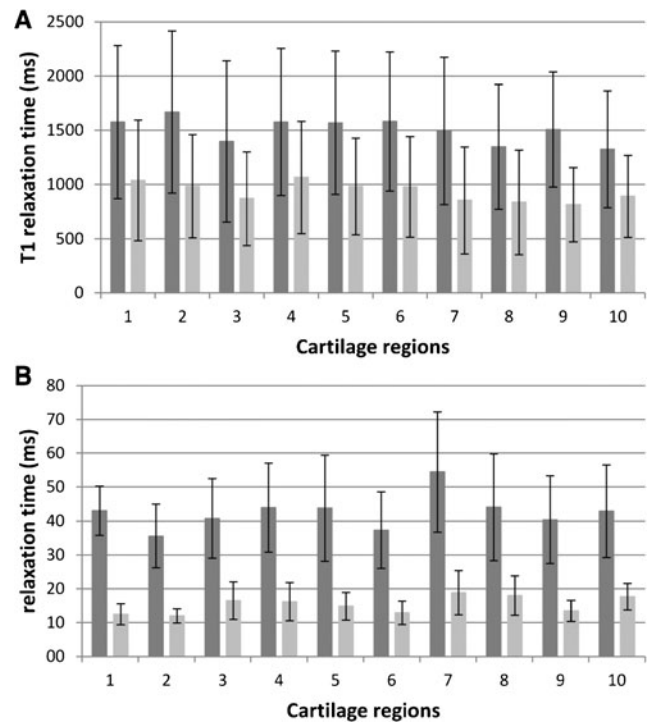


Fig. 4 **a** Means of $T1_0$ (dark grey) and $T1_{\text{Gd}}$ (light grey) over the different evaluated cartilage regions with standard deviations. **b** Means of T2 (dark grey) and $T2^*$ (light grey) relaxation times over the different evaluated cartilage regions with standard deviations. See Fig. 1 for the exact locations of the placed ROIs (1 acetabulum lateral slice, 2 femur lateral slice, 3 acetabulum central slice ventral, 4 femur central slice ventral, 5 acetabulum central slice central, 6 femur central slice central, 7 acetabulum central slice dorsal, 8 femur central slice dorsal, 9 acetabulum medial slice, 10 femur medial slice)

reader reliability: mean bias 0.5 ms (95 % CI -0.9 to 1.8 ms), CV 13 %; inter-reader reliability: mean bias 0.0 ms (95 % CI -0.8 to 0.8 ms), CV 7.6 %).

Figure 5 gives an impression of image quality comparing T1, T2 and $T2^*$ relaxation time maps and shows the T2 map

Table 2 T1 relaxation times calculated by using the inversion recovery sequence ($T1_{\text{calc}}$) in five different subjects without and with contrast enhancement (Gd) in comparison to the ones measured in the relaxation time maps with the dual-flip-angle technique ($T1_{\text{DFA}}$)

	$T1_{\text{zero}}$ (ms)	$T1_{\text{calc}}$ (ms)	$T1_{\text{DFA}}$ (ms)	$T1_{\text{calc}} / T1_{\text{DFA}}$
Subject 1, no Gd	800	1154	1144	0.99
Subject 2, no Gd	500	721	777	1.07
Subject 3, no Gd	800	1154	1229	1.06
Subject 4+Gd	500	721	734	1.02
Subject 5+Gd	600	866	903	1.04
Mean	600	923	957	1.04

$T1_{\text{zero}}$ is the inversion time with the lowest signal intensity in cartilage and $T1_{\text{calc}} = T1_{\text{zero}} / \ln 2$. Measurements both for $T1_{\text{zero}}$ and $T1_{\text{DFA}}$ were done in corresponding central slices of the hip joint in sagittal view by placing an ROI in the central part of the cartilage, including both the acetabular and femoral components

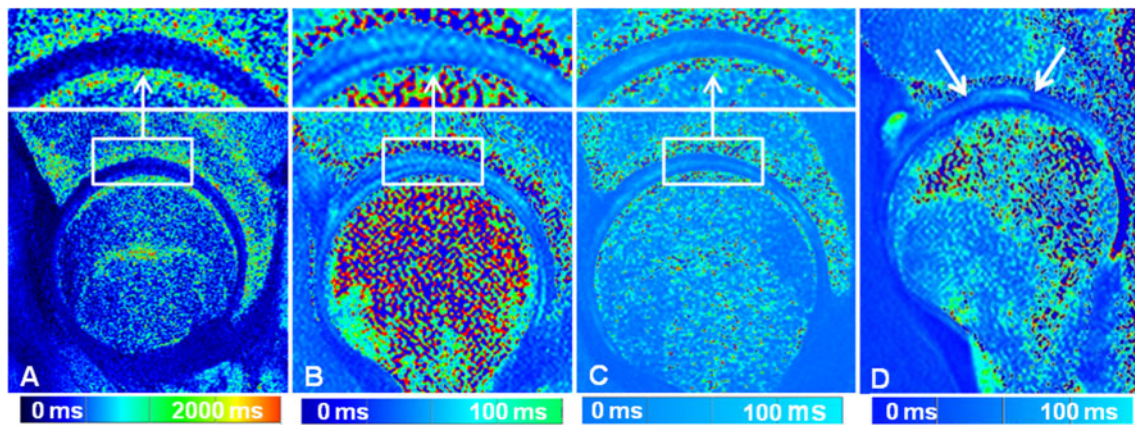


Fig. 5 Contrast-enhanced T1 relaxation time map (**a**) as well as unenhanced T2 (**b**) and T2* (**c**) relaxation time maps of the hip joint in three different volunteers in sagittal view; enlarged views of the joint space are shown above. Note the clear differentiation between

acetabular and femoral cartilage. **d** Sagittal T2 relaxation time map of a patient 10 months after acetabular cartilage transplantation with clearly higher T2 relaxation times in the transplanted region (*between the arrows*) compared to the adjacent healthy cartilage

of a patient imaged 10 months after acetabular cartilage transplantation.

Discussion

In this initial study on healthy volunteers, quantitative MRI techniques were applied for hip cartilage imaging at 7 T with diagnostic image quality. The high spatial resolution gained at 7 T yielded a good to excellent delineation of acetabular and femoral cartilage in T1, T2 and T2* relaxation time maps, which is essential for the evaluation of cartilage pathologies. In previous studies at lower field strengths the spatial resolution of cartilage mapping sequences was restricted as a result of SNR limitations [28], and Siversson et al. reported problems with exactly delineating acetabular and femoral cartilage [29]. As this delineation is a major requirement to identify pathologies of hip cartilage, the higher field strength of 7 T with the possibility of higher spatial resolution owing to increased SNR offers an applicable solution for imaging these critical structures. Furthermore, the very homogenous signal in the hip joint region as well as the predominant absence of artefacts in this study resulted in high quality images, indicating that the techniques would be applicable in patient studies as well, as shown for one exemplary patient after acetabular cartilage transplantation. Another very important practical factor for implementing in particular dGEMRIC in clinical routine is the omission of time-consuming pre-contrast T1 mapping. As shown for lower field strengths [30, 31], our results showing high correlation between $T1_{Gd}$ and $R1_{\Delta}$ suggest that pre-contrast T1 mapping is dispensable at 7 T as well.

As, to the best of our knowledge, other studies on relaxation times of hip cartilage at 7 T do not exist, the results of this study can only be discussed in the context of 7 T studies focused on the knee and in the context of hip imaging at lower field strengths. Pakin et al. [18] reported on native T1

relaxation times of knee cartilage at 7 T that are comparable to the results of the present study. Welsch et al. [17] observed markedly lower T1 relaxation times after performing dGEMRIC at 7 T in healthy knees. However, as a result of the small number of subjects examined (five each) and influencing factors like age and BMI, the confidence of these comparisons is weak. As T1 increases with the field strength [32], T1 relaxation times measured at 7 T in this study were clearly higher compared to 1.5 T and 3 T studies [33, 34]. For T2 and T2* relaxation times at 7 T, Welsch et al. [17, 19] and Chang et al. [20] reported on values in knee cartilage that are comparable to the present results. T2 and T2* relaxation times of hip cartilage examined at 1.5 T and 3 T were mostly higher than the current results [35]. The high correlation between T2 and T2* values in the present study also underlines the robustness of the applied methods.

In this study, a wide range of T1 relaxation times were apparent between individuals. However, values were of the same order over the different evaluated cartilage regions intra-individually, and concordantly observable both before and after contrast agent administration. Hence, the volunteers themselves may have been the source of this variation. As we just asked for disorders affecting the hip but did not include a detailed clinical examination, the results might have been biased by unknown hip pathologies as well as asymptomatic changes in cartilage composition. Technical reasons such as noise, partial volume effects or residual B1+ heterogeneities cannot be fully neglected but are considered unlikely because of the aforementioned intra-individual correlations. Furthermore, the validity of measuring the T1 relaxation times using the dual-flip-angle technique was confirmed by applying an inversion recovery sequence in several individuals, verifying the accuracy of the measured values. In subsequent studies on patients with cartilage defects or after cartilage repair surgery we recommend to use standardized relaxation ratios, as reported by other groups [36, 37], to gain inter-individual

comparability. However, as in our healthy study population no discrimination could be made between “healthy” and “injured” cartilage, a reasonable standardization was not possible.

As shown previously by Bittersohl et al. [38], a specific zonal variation of T1 relaxation times exists as a result of the higher content of glycosaminoglycans in the weight-bearing area of the joint [39] and topographic variation was also shown for T2 relaxation times at 3 T [40]. Although significant differences of T2 and T2* relaxation times between individual regions were found in the present study as well, no specific pattern regarding the anatomical distribution of these differences could be identified. The most likely reason for this is the comparably small study group in combination with the high inter-individual variance of relaxation times mentioned above. Furthermore, as sagittal 2D relaxation maps were acquired, the lateral and medial ROIs were placed only 5–10 mm away from the central slice, which might not have been enough to really include peripheral joint regions. Further limitations include the limited number of volunteers examined and the manual approach for drawing the ROIs. However, owing to the high intra- and inter-reader reliability, we trust the accuracy of these measurements.

In conclusion, the presented results show the technical feasibility of T1, T2 and T2* mapping of hip cartilage at 7 T MRI with diagnostic image quality. Especially for the application in subsequent clinical studies on patients, it is notable that pre-contrast T1 mapping can be omitted from a dGEMRIC protocol at 7 T.

Acknowledgments The authors thank Desmond Tse (Maastricht University, The Netherlands) for providing the source code of the DREAM sequence.

This work was supported by a research grant of the University Duisburg-Essen, Germany, awarded to the first author.

The scientific guarantor of this publication is Dr. med. Andrea Lazik. The authors of this manuscript declare no relationships with any companies whose products or services may be related to the subject matter of the article. This study has received funding from the University of Duisburg-Essen: A research grant (“IFORES”) was awarded to the first author. No complex statistical methods were necessary for this paper. Institutional review board approval was obtained. Written informed consent was obtained from all subjects (patients) in this study. No study subjects or cohorts have been previously reported. Methodology: prospective, experimental, performed at one institution.

References

- Rogers AD, Payne JE, Yu JS (2013) Cartilage imaging: a review of current concepts and emerging technologies. *Semin Roentgenol* 48:148–157
- Sanghvi D, Munshi M, Pardiwala D (2014) Imaging of cartilage repair procedures. *Indian J Radiol Imaging* 24:249–253
- Mosher TJ, Walker EA, Petscavage-Thomas J, Guermazi A (2013) Osteoarthritis year 2013 in review: imaging. *Osteoarthritis Cartilage* 21:1425–1435
- Bashir A, Gray ML, Burstein D (1996) Gd-DTPA2- as a measure of cartilage degradation. *Magn Reson Med* 36:665–673
- Burstein D, Velyvis J, Scott KT et al (2001) Protocol issues for delayed Gd(DTPA)(2-)-enhanced MRI (dGEMRIC) for clinical evaluation of articular cartilage. *Magn Reson Med* 45:36–41
- Binks DA, Hodgson RJ, Ries ME et al (2013) Quantitative parametric MRI of articular cartilage: a review of progress and open challenges. *Br J Radiol* 86:20120163
- Kijowski R (2010) Clinical cartilage imaging of the knee and hip joints. *AJR Am J Roentgenol* 195:618–628
- Krug R, Stehling C, Kelley DA, Majumdar S, Link TM (2009) Imaging of the musculoskeletal system in vivo using ultra-high field magnetic resonance at 7 T. *Invest Radiol* 44:613–618
- Hoult DI, Phil D (2000) Sensitivity and power deposition in a high-field imaging experiment. *J Magn Reson Imaging* 12:46–67
- Mao W, Smith MB, Collins CM (2006) Exploring the limits of RF shimming for high-field MRI of the human head. *Magn Reson Med* 56:918–922
- Van de Moortele PF, Akgun C, Adriany G et al (2005) B(1) destructive interferences and spatial phase patterns at 7 T with a head transmitter array coil. *Magn Reson Med* 54:1503–1518
- Orzada S, Quick HH, Ladd ME et al (2009) A flexible 8-channel transmit/receive body coil for 7 T human imaging. 17th Scientific Meeting ISMRM, Hawaii, USA, pp 2999
- Ellermann J, Goerke U, Morgan P et al (2012) Simultaneous bilateral hip joint imaging at 7 Tesla using fast transmit B(1) shimming methods and multichannel transmission - a feasibility study. *NMR Biomed* 25:1202–1208
- Chang G, Deniz CM, Honig S et al (2014) MRI of the hip at 7T: feasibility of bone microarchitecture, high-resolution cartilage, and clinical imaging. *J Magn Reson Imaging* 39:1384–1393
- Theyssohn JM, Kraff O, Orzada S et al (2013) Bilateral hip imaging at 7 Tesla using a multi-channel transmit technology: initial results presenting anatomical detail in healthy volunteers and pathological changes in patients with avascular necrosis of the femoral head. *Skeletal Radiol* 42:1555–1563
- Theyssohn JM, Kraff O, Theyssohn N et al (2014) Hip imaging of avascular necrosis at 7 Tesla compared with 3 Tesla. *Skeletal Radiol* 43:623–632
- Welsch GH, Mamisch TC, Hughes T et al (2008) In vivo biochemical 7.0 Tesla magnetic resonance: preliminary results of dGEMRIC, zonal T2, and T2* mapping of articular cartilage. *Invest Radiol* 43:619–626
- Pakin SK, Cavalcanti C, La Rocca R, Schweitzer ME, Regatte RR (2006) Ultra-high-field MRI of knee joint at 7.0T: preliminary experience. *Acad Radiol* 13:1135–1142
- Welsch GH, Apprich S, Zbyn S et al (2011) Biochemical (T2, T2* and magnetisation transfer ratio) MRI of knee cartilage: feasibility at ultra-high field (7T) compared with high field (3T) strength. *Eur Radiol* 21:1136–1143
- Chang G, Xia D, Sherman O et al (2013) High resolution morphologic imaging and T2 mapping of cartilage at 7 Tesla: comparison of cartilage repair patients and healthy controls. *MAGMA* 26:539–548
- Nehrke K, Bornert P (2012) DREAM—a novel approach for robust, ultrafast, multislice B(1) mapping. *Magn Reson Med* 68:1517–1526
- Kraff O, Lazik A, Brenner D et al (2015) In vivo comparison of B1 mapping techniques for hip joint imaging at 7 Tesla. 23rd Scientific Meeting ISMRM, Toronto, Canada
- Manuel A, Li W, Jellus V, Hughes T, Prasad PV (2011) Variable flip angle-based fast three-dimensional T1 mapping for delayed gadolinium-enhanced MRI of cartilage of the knee: need for B1 correction. *Magn Reson Med* 65:1377–1383
- Siversson C, Chan J, Tiderius CJ et al (2012) Effects of B1 inhomogeneity correction for three-dimensional variable flip angle T1

- measurements in hip dGEMRIC at 3 T and 1.5 T. *Magn Reson Med* 67:1776–1781
25. Deoni SC, Rutt BK, Peters TM (2003) Rapid combined T1 and T2 mapping using gradient recalled acquisition in the steady state. *Magn Reson Med* 49:515–526
 26. Fram EK, Herfkens RJ, Johnson GA et al (1987) Rapid calculation of T1 using variable flip angle gradient refocused imaging. *Magn Reson Imaging* 5:201–208
 27. Noel P, Bammer R, Reinhold C, Haider MA (2009) Parallel imaging artifacts in body magnetic resonance imaging. *Can Assoc Radiol J* 60:91–98
 28. Lazik A, Korsmeier K, Classen T et al (2014) 3 Tesla high-resolution and delayed gadolinium enhanced MR imaging of cartilage (dGEMRIC) after autologous chondrocyte transplantation in the hip. *J Magn Reson Imaging*. doi:10.1002/jmri.24821
 29. Siversson C, Akhondi-Asl A, Bixby S, Kim YJ, Warfield SK (2014) Three-dimensional hip cartilage quality assessment of morphology and dGEMRIC by planar maps and automated segmentation. *Osteoarthritis Cartilage* 22:1511–1515
 30. Bittersohl B, Hosalkar HS, Kim YJ, Werlen S, Siebenrock KA, Mamisch TC (2009) Delayed gadolinium-enhanced magnetic resonance imaging (dGEMRIC) of hip joint cartilage in femoroacetabular impingement (FAI): are pre- and postcontrast imaging both necessary? *Magn Reson Med* 62:1362–1367
 31. Williams A, Mikulis B, Krishnan N, Gray M, McKenzie C, Burstein D (2007) Suitability of T(1Gd) as the dGEMRIC index at 1.5T and 3.0T. *Magn Reson Med* 58:830–834
 32. Rooney WD, Johnson G, Li X et al (2007) Magnetic field and tissue dependencies of human brain longitudinal 1H2O relaxation in vivo. *Magn Reson Med* 57:308–318
 33. Zilkens C, Miese F, Kim YJ et al (2012) Three-dimensional delayed gadolinium-enhanced magnetic resonance imaging of hip joint cartilage at 3T: a prospective controlled study. *Eur J Radiol* 81:3420–3425
 34. Bittersohl B, Hosalkar HS, Haamberg T et al (2009) Reproducibility of dGEMRIC in assessment of hip joint cartilage: a prospective study. *J Magn Reson Imaging* 30:224–228
 35. Bittersohl B, Miese FR, Hosalkar HS et al (2012) T2* mapping of acetabular and femoral hip joint cartilage at 3 T: a prospective controlled study. *Invest Radiol* 47:392–397
 36. Lattanzi R, Petchprapa C, Glaser C et al (2012) A new method to analyze dGEMRIC measurements in femoroacetabular impingement: preliminary validation against arthroscopic findings. *Osteoarthritis Cartilage* 20:1127–1133
 37. Trattnig S, Ohel K, Mlynarik V, Juras V, Zbyn S, Komer A (2015) Morphological and compositional monitoring of a new cell-free cartilage repair hydrogel technology - GelinC by MR using semi-quantitative MOCART scoring and quantitative T2 index and new zonal T2 index calculation. *Osteoarthritis Cartilage*. doi:10.1016/j.joca.2015.07.007
 38. Bittersohl B, Hosalkar HS, Werlen S, Trattnig S, Siebenrock KA, Mamisch TC (2011) dGEMRIC and subsequent T1 mapping of the hip at 1.5 Tesla: normative data on zonal and radial distribution in asymptomatic volunteers. *J Magn Reson Imaging* 34:101–106
 39. Yoshida K, Azuma H (1982) Contents and compositions of glycosaminoglycans in different sites of the human hip joint cartilage. *Ann Rheum Dis* 41:512–519
 40. Watanabe A, Boesch C, Siebenrock K, Obata T, Anderson SE (2007) T2 mapping of hip articular cartilage in healthy volunteers at 3T: a study of topographic variation. *J Magn Reson Imaging* 26:165–171